Thermochimica Acta 496 (2009) 1–12

Contents lists available at ScienceDirect

Thermochimica Acta

journal homepage: www.elsevier.com/locate/tca

Review

Evaluation of decomposition kinetics of energetic materials in the combustion wave

V.P. Sinditskii*, V.Yu. Egorshev, V.V. Serushkin, A.I. Levshenkov, M.V. Berezin, S.A. Filatov, S.P. Smirnov

Mendeleev University of Chemical Technology, 9 Miusskaya Square, 125047 Moscow, Russia

ARTICLE INFO

Article history:
Received 29 April 2009
Received in revised form 6 July 2009
Accepted 10 July 2009
Available online 21 July 2009

Keywords:
Energetic materials
Decomposition kinetics
Propellant oxidizers
Nitramines
Heterocyclic compounds
Vapor pressure
Surface temperature

ABSTRACT

Experimental data on burning rates and surface temperatures have been shown to allow deriving unique information on decomposition kinetics of energetic materials at high temperatures, provided combustion of these materials occurs in the condensed phase. In the paper, kinetic parameters of the leading reaction on combustion of four solid rocket propellant oxidizers: ammonium perchlorate (AP), ammonium nitrate (AN), ammonium dinitramide (ADN), and hydrazine nitroformate (HNF), as well as six energetic fillers: 1,3,5,7-tetranitro-1,3,5,7-tetraazacyclooctane (HMX), 1,3,5-trinitro-1,3,5-triazacyclohexane (RDX), bicyclo-1,3,5,7-tetranitro-l,3,5,7-tetraazacyclooctane (bicyclo-HMX), hexanitrohexaazaisowurtzitane (CL-20), 3,3′-diamino-4,4′-azofurazan (DAAzF), and 3-nitro-l,2,4-triazole-5-one (NTO) are evaluated from available combustion data.

Contents

1. Introduction

Experimental evaluation of kinetic parameters of energetic materials decomposition at temperatures higher than 300–350 °C by using general methods based on monitoring sample mass change, heat or gas evolution, usually involves difficulties connected with very short conversion time. For example, time of half-decomposition of ordinary explosives such as RDX at 350 °C is not more than 0.0002 s, that is far below capabilities of existing recording devices.

The condensed phase of a burning energetic material is heated up to temperatures 250–1000 °C that can be recorded using microthermocouple technique with accuracy of 5–20 °C depending on the material nature and experimenter experience. Decreasing pressure leads in widening combustion wave zones, making measurements more accurate. At the same time, the burning rate measurements are usually feasible with an experimental error less than 5%. Using experimental data on burning rates and surface temperatures one can derive rate constants of the leading reaction from an adequate combustion model.

In the paper, experimental data on burning rates and surface temperatures for a series of energetic materials from different

* Corresponding author at: Department of Chemical Engineering, Mendeleev University of Chemical Technology, 9 Miusskaya Square, 125047 Moscow, Russia.
Tel.: +7 495 4966027; fax: +7 495 4966027.
E-mail address: vps@rctu.ru (V.P. Sinditskii).

0040-6031/$ – see front matter © 2009 Elsevier B.V. All rights reserved.
doi:10.1016/j.tca.2009.07.004

classes, such as onium salts (AP, AN, ADN, HNF), nitramines (HMX, RDX, bicyclo-HMX, CL-20), and heterocyclic compounds (NTO, DAAzF) were used to determine decomposition kinetics in the combustion wave.

2. Experimental

Syntheses of the substances, sample preparation technique, burning rate and thermocouple measurements are described in related papers, which are referred to in the text.

Most of burning rate measurements were carried out in a constant pressure window bomb with a volume of 1.5 l. Temperature profiles in the combustion wave were measured using fine Π-shaped thermocouples. The thermocouples were welded from 80% tungsten + 20% rhenium and 95% tungsten + 5% rhenium wires 20 μm in diameter and rolled into bands 7 μm thick. The thermocouple was embedded in the center of the strand so that the section with the junction was parallel to the combustion front.

3. Results and discussion

3.1. Theory

Decomposition of an energetic material begins with endothermic rupture of the weakest bond in the molecule. Subsequent secondary radical reactions have significantly less activation energy. A difference in the activation energies results in the leading reaction on combustion to be either initial endothermic decomposition of the original material to form active species or subsequent secondary heat-generating reactions, depending on the temperature interval. In the interval of 150–300 °C, within which thermal decomposition of energetic materials is most often studied, the limiting stage is usually characterized by high activation energy, with the secondary reactions being of low activation energy and proceeding fast. Associated autocatalytic processes can interfere in correct determination of kinetic parameters of bond cleavage, but are of insignificant importance in the combustion wave at high temperatures because of low activation energies of such reactions.

As temperature increases, secondary radical reactions get slower than the primary decomposition of the molecule, thus becoming rate-limiting ones in the heat generation process. Since the burning rate is determined by heat-release kinetics, the leading role can be switched to the secondary radical reactions starting from certain temperatures. Calculations [1], confirmed by experimental observations [2] show that this transition temperature is in the interval of 1000–1500 °C for nitrocompounds and above 2500 °C for endothermic substances such as organic azides. These temperatures lie above normal surface temperatures, suggesting that the rate-limiting process in the condensed phase of a burning substance is for the most part primary bond-cleavage reactions.

It may be supposed therefore that the decomposition kinetics of a substance can be derived from its burning rate data if combustion is governed by condensed-phase reactions. In order for kinetic parameters of the rate-controlling reaction could be evaluated from available experimental data on burning rates and surface temperatures, an adequate combustion model must be chosen and considered.

Several combustion models with condensed-phase priority have created in the Soviet Union starting from the forties of past century. Zeldovich, one of the authors of the combustion model for gases and volatile explosives [3], proposed an expression for propagation of the exothermic reaction wave in the condensed phase of energetic materials. The equation was derived assuming the concentration of a reacting substance in the reaction zone equal to initial one, i.e., the degree of conversion was assumed to be small:

$$m = \sqrt{\frac{2\rho^2 \chi Q}{c_p(T_s - T_0 + L_m/c_p)^2}\left(\frac{RT_s^2}{E}\right) \cdot A \cdot e^{-E/RT_s}} \quad (1)$$

where c_p, ρ, χ are specific heat, density, and thermal diffusivity of the condensed phase, T_s and Q are the surface temperature and heat effect, E and A are activation energy and preexponential factor of the leading reaction in the condensed phase. The expression $T_s - T_0 + L_m/c_p$ accounts for warming-up of the condensed phase from initial temperature, T_0, to surface temperature, T_s, and melting, where L_m is heat of melting.

In the subsequent years, a number of elementary condensed-phase combustion models were proposed and were summarized in Ref. [4]. According to Ref. [4], all the models can be divided into two groups. The first one includes models that consider full conversion of the substance in the combustion wave, i.e., when the reaction proceeds at the maximum combustion temperature $T_{max} = T_0 + Q/c_p$. This type of models was developed in theoretical works by Novozhilov [5] and Khaikin and Merzhanov [6]. The burning rate here is independent of pressure, making these models suitable for describing combustion of materials which do not evaporate and do not produce gases at burning.

The modes of the second group consider formation of the burning surface of different physico-chemical nature. The value of T_s and degree of decomposition in the condensed phase, η, reflect the incompleteness of conversion ($T_s < T_{max}$, $\eta < 1$) and determine the burning rate. Gas-phase reactions do not influence the rate of combustion and are not included into consideration. The burning surface of such materials is a result of dispersion or evaporation of the condensed phase [6–9]. As compared to Zeldovich's model [3], models developed in works [8–10] operate with different kinetic equations of heat generation process: zero-, first-, second-order reactions can be used. These models comply with the Zeldovich's equation for the zero-order reaction or, more specifically, for the first-order reaction with no change of the concentration in the reaction zone. If change in the concentration is taken into account, the first-order constant calculated with these models will grow 1.2–1.8 times depending on the degree of conversion in the condensed phase.

According to the models, the degree of conversion of energetic materials in the condensed phase is defined as the ratio between heat needed to warm up a material to the surface temperature, taking into account heat of modification and phase changes, and heat effect of the decomposition reaction. A part of the substance remains undecomposed at the surface and is ejected into the gas phase with flying-off gases. The following decomposition and evaporation of droplets does not exert essential influence on the burning rate.

The above model is most suitable for describing combustion of different energetic materials capable of evaporation, providing correct boundaries of application area. Flameless combustion, which obeys to the model best, is usually observed at low pressures. As pressure grows a high-temperature flame arises, and a judgment about location of the leading reaction can be done by analyzing temperature profiles of the combustion wave. It is generally believed that the leading role belongs to the condensed phase if the heat flux from the gas to the burning surface is negligibly small [11]. In addition, the model can be employed also in the case of substantial heat flux if the heat feedback, Q_g, is less than or comparable to the heat necessary for evaporation of unreacted in the condensed phase substance, $(1-\eta)Q_{ev}$. In this case, all the heat Q_g is consumed for evaporation of the dispersal phase above the surface, having no effect on the burning rate, which is determined by expression (1).

In the general case that the heat feedback from the gas becomes superior over the heat required for evaporation, the expression (1)

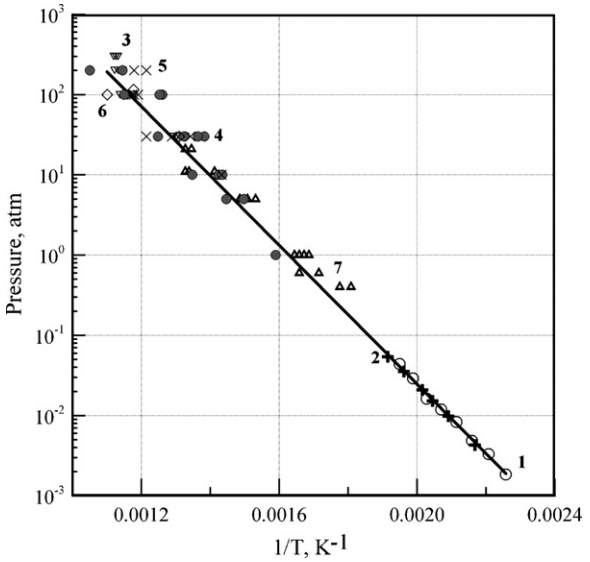

Fig. 1. Relationship between pressure and dissociation temperature of ammonium nitrate. Gas pressure above molten AN (1 [18] and 2 [17]), surface temperatures on burning of AN (3) and AN-based propellants: AN/HTPB (4), AN/AP/HTPB (5), and AN/AP/Al/HTPB (6) at different pressures. Points (7) relate to surface temperatures of ADN [20].

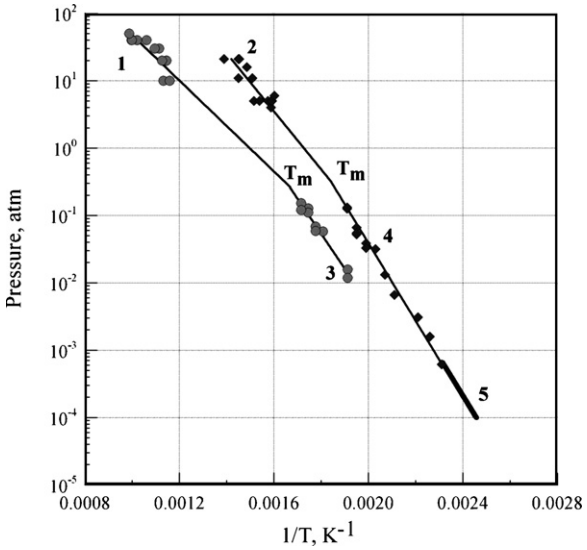

Fig. 2. Vapor pressure as a function of reciprocal temperature: surface temperatures of DAAzF (1) and NTO (2) at different pressures, initial pressures in glass Bourdon gauges at decomposition of solid DAAzF (3) and NTO (4), vapor pressure above solid NTO calculated from Ref. [27] (line 5).

cannot be longer suitable for describing the burning rate, even if the condensed-phase priority still remains. For this case several combustion models have been created such as Merzhanov–Dubovitskii model [12], or a model proposed in paper of Ward et al. [13]. In order to evaluate the decomposition kinetics of energetic materials which combustion obeys these models, the heat flux from the gas phase needs to be known additionally. It complicates considerably the task of evaluation of kinetic parameters from combustion data, and we did not consider this case in our work.

3.2. Temperature measurements

To calculate kinetic parameters of the leading reaction, it is necessary to know heat effect in the condensed phase and thermophysical properties of the reaction zone. Errors of measurements of these values as well as using averaged parameters exert some effect on the accuracy of rate constant calculations. However, the surface temperature measurement error causes the most significant error of calculated constants and activation energies; the latter can be as large as 10 kcal mole^{-1}. Our numerous thermocouple-aided experimental studies on combustion of different energetic materials have shown that a material in the condensed phase can be heated up to its maximum temperature – boiling point or, in the case of salts, dissociation temperature. This circumstance provides possibility to resort to known temperature dependences of vapor pressures along with experimental data on surface temperatures to describe the temperature–pressure relation in a widened pressure interval and, thus, significantly reduce a possible error.

Typical plots of pressure dependences of the surface temperature combined with data on vapor pressures are presented in Figs. 1–6.

Temperature distributions in the combustion wave of AN-based compositions were studied in several works. In Ref. [14] it was shown that the surface temperature of catalyzed ammonium nitrate (2.5% CrO_3) remained constant and equal to 576 ± 12 K over a wide pressure range (from 7 to 30 MPa). This result is strange in light of the data on surface temperatures of other onium salts, and is apparently caused by some methodological mistake.

The existence of pressure dependence of the surface temperature was found for AN mixtures with catalytic additives of 5% of KCl and 4% of charcoal within a pressure interval of 1.5–5 MPa [15], as well as for AN mixtures containing 4% of $K_2Cr_2O_7$ [16].

The surface temperatures measured for AN and AN-based propellants [15,16] are shown in Fig. 1. Also presented there are data on gas pressure above the AN liquid phase taken from Refs. [17,18] and surface temperatures of ADN, which were shown in Refs. [19,20] to correspond to the dissociation temperature of AN, a product of ADN decomposition in the condensed phase. As can be seen from Fig. 1, the surface temperatures obtained for different mixtures of AN as well as the surface temperatures of ADN are located in vicinity of a straight line of gas pressure above liquid AN.

Using temperatures taken from the fitting line instead of experimental data obviously results in an essential decrease in error of kinetic parameters calculations.

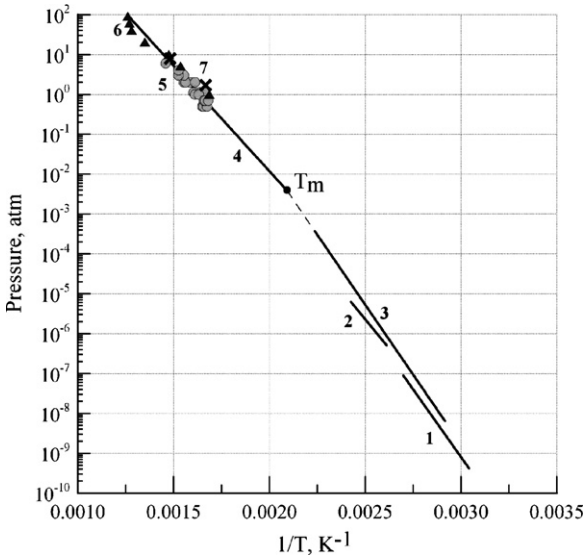

Fig. 3. Vapor pressure as a function of reciprocal temperature: vapor pressure above solid RDX (1 [28], 2 [29], and 3 [30]), vapor pressure above melted RDX (4, calculated from Ref. [30]), and RDX surface temperatures (5 present work, 6 [31] and 7 [32]) at different pressures.

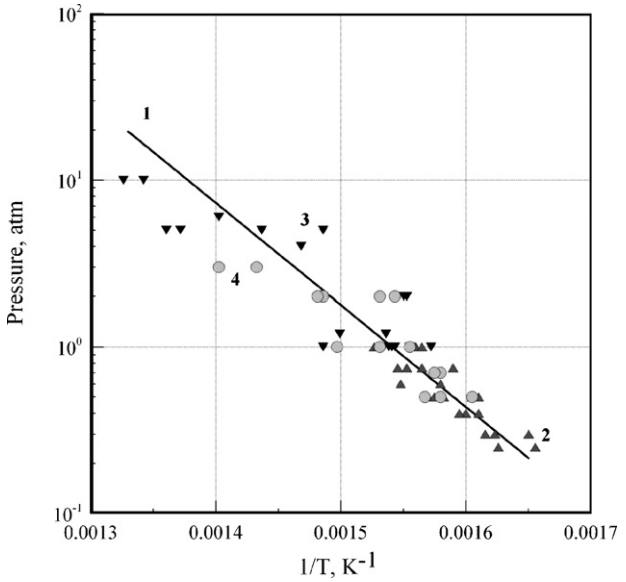

Fig. 4. Vapor pressure as a function of reciprocal temperature: vapor pressure above liquid HMX (1 calculated in Ref. [47]), surface temperatures of phlegmatized HMX (2 [47]), crystalline HMX (3 [47]), and bicyclo-HMX (4 [48]) at different pressures.

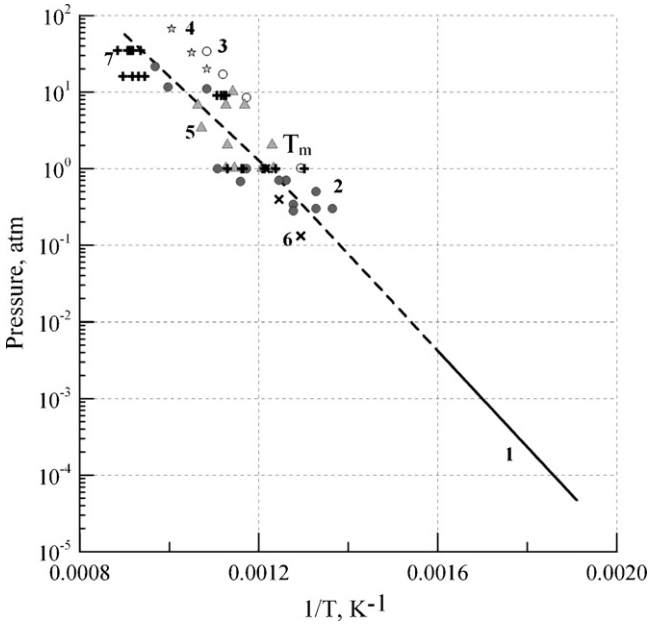

Fig. 6. Pressure dependence of the surface temperature for AP-based mixtures obtained in thermocouple-aided measurements (2 [49], 5 [50], 6 [51], 7 [52] and burning surface pyrometry (3 and 4 [53]). The solid and dashed lines represent equilibrium gas pressure over solid (1 [54]) and melted AP surface.

In the case of AN, temperature dependence of gas pressure and dependence of T_s on pressure both are measured for the substance in the same phase state. In the case of high-melting substances, data on temperature dependence of vapor pressure are usually obtained for the solid state, whereas the surface temperature of a burning material relates to the liquid material. Nevertheless, low-temperature data on vapor pressure help to determine the surface temperature more precisely. The fact is that an intersection of vapor pressure lines above liquid and solid substance is the melting point. Therefore, extrapolation of the temperature dependence of vapor pressure over a solid energetic material to the melting point allows widening temperature interval of vapor pressure over liquid. The slope of the temperature dependence of vapor pressure over substance is determined by the phase transition heat effect: heat of sublimation over solid and heat of vaporization over liquid. The difference between them corresponds to the heat of melting. Knowing heat of vaporization, one can obtain more correct description of the burning material surface temperature as a function of pressure.

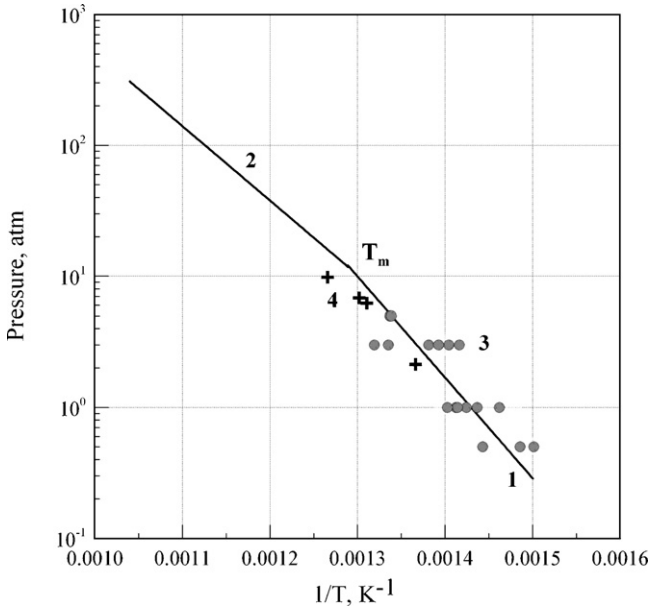

Fig. 5. Vapor pressure as a function of reciprocal temperature: vapor pressure above solid (1) and liquid CL-20 (2), and CL-20 surface temperatures (3 [61] and 4 [62]) at different pressures.

Examples of adjustment of $P(T_s)$ dependences for NTO and DAAzF starting from sublimation data are presented in Fig. 2. Using experimental data on surface temperatures and vapor pressures above solid DAAzF, measured in glass manometers (Bourdon gauge) as onset pressure rise in the gauge at low temperatures (sublimation) [21], one can describe the vapor pressure of DAAzF in the liquid and solid phases (see Fig. 2). Melting point (T_m) is an intersection of two straight lines, fitting high- and low-temperature data.

In the case of NTO, data on vapor pressure are shown together with thermocouple data in the high-temperature region and Bourdon gauge data in the low-temperature region [22]. A heat of NTO vaporization (82.4 kJ mole^{-1} or 19.7 kcal mole^{-1}) was obtained as a difference between a heat of sublimation of 110.5 kJ mole^{-1} (26.4 kcal mole^{-1}) and a heat of melting of 28.0 kJ mole^{-1} (6.7 kcal mole^{-1}). A heat of sublimation was calculated from enthalpies of formation of solid (129.4 kJ mole^{-1} or 30.93 kcal mole^{-1}) [23] and gaseous NTO (13.4 and 23.8 kJ mole^{-1} (3.2 and 5.7 kcal mole^{-1}) [24,25]). A heat of melting of 28.0 kJ mole^{-1} (6.7 kcal mole^{-1}, 51.5 cal g^{-1}) was calculated from NTO solubility in nitric acid solutions [26]. The dependence of NTO boiling temperature on pressure is presented in Fig. 2, which shows a good correlation between experimental surface temperatures in the interval of 0.4–2.1 MPa and the theoretical dependence of NTO boiling temperature on pressure, calculated using heat of vaporization and experimental boiling temperature at 0.5 MPa.

The temperature dependence of vapor pressure above solid NTO was obtained using initial vapor pressures of NTO measured in glass Bourdon gauge experiments on NTO decomposition and the heat of sublimation as 110.5 kJ mole^{-1} (26.4 kcal mole^{-1}), calculated earlier from thermodynamic data [23,25], or 107.9 kJ mole^{-1} (25.8 kcal mole^{-1}), calculated from experimental data [27]. Crossing of two straight lines in the melting point is a good confirmation of these calculations.

Table 1
Thermodynamic data on evaporation and sublimation of studied energetic materials.

Substance	State of matter	Temperature interval (K)	Temperature dependence of pressure above condensed phase (pressure in atm)	Heat of evaporation (or sublimation) (kJ mole^{-1})	References
AP	Solid	523–623	$\ln P = 17.614 - 14{,}468.8/T$	(240.6)	[54]
	Liquid	820–1100	$\ln P = 15.425 - 12{,}649.7/T$	210.5	This work
AN	Liquid	442–552	$\ln P = 16.329 - 10{,}031.7/T$	166.9	[17]
ADN	Liquid	580–750	$\ln P = 16.329 - 10{,}031.7/T$	166.9	[20]
HNF	Liquid	550–750	$\ln P = 17.03 - 9909/T$	164.8	This work
RDX	Solid	343–447	$\ln P = 28.216 - 16{,}143.4/T$	(134.3)	[30]
	Liquid	590–795	$\ln P = 19.925 - 12{,}179.2/T$	101.3	This work
HMX	Liquid	600–835	$\ln P = 21.717 - 14{,}091.6/T$	117	[47]
Bicyclo-HMX	Liquid	630–690	$\ln P = 21.717 - 14{,}091.6/T$	117	This work
CL-20	Solid	660–775	$\ln P = 25.328 - 17{,}715.1/T$	(147.3)	This work
	Liquid	775–960	$\ln P = 19.337 - 13{,}085/T$	108.8	This work
NTO	Solid	523–599	$\ln P = 23.326 - 13{,}286.4/T$	(110.5)	[22]
	Liquid	599–1015	$\ln P = 17.123 - 9914.4/T$	82.4	[22]
DAAzF	Solid	523–599	$\ln P = 18.610 - 11{,}963.6/T$	(99.6)	[21]
	Liquid	599–1015	$\ln P = 11.623 - 7758.8/T$	64.4	[21]

Similarly, pressure dependence of the surface temperature was obtained for RDX and other substances. Sublimation data for RDX measured in [28–30] are presented in Fig. 3. Also shown in Fig. 3 are RDX surface temperatures measured in works [31,32] and in our laboratory. As seen from Fig. 3, the surface temperatures fall on the evaporation line, which has been calculated as in Ref. [30], with the heat of melting (33.1 kJ mole^{-1} or 7.9 kcal mole^{-1} [33]) taken into account.

In the case of HNF, the only enthalpy of sublimation of 193.7 kJ mole^{-1} (46.3 kcal mole^{-1}) was measured in the temperature interval of 34.4–67.7 °C [34]. This value is in a good agreement with the enthalpy of HNF dissociation ΔH_{diss} (196.19 kJ mole^{-1} or 46.89 kcal mole^{-1}) calculated from enthalpies of formation of the solid salt (−76.86 kJ mole^{-1} or −18.37 kcal mole^{-1} [35]), gaseous hydrazine (95.19 kJ mole^{-1} or 22.75 kcal mole^{-1} [36]), and trinitromethane (24.27 kJ mole^{-1} or 5.8 kcal mole^{-1} [37]). The enthalpy of evaporation of liquid HNF (184.9 kJ mole^{-1} or 44.2 kcal mole^{-1}) can be calculated as the enthalpy of sublimation minus enthalpy of melting (estimated value 11.3 kJ mole^{-1} or 2.7 kcal mole^{-1}).

Experimental data on T_s [38], if plotted in the coordinates pressure *vs.* reciprocal temperature, yield the enthalpy of the salt dissociation ΔH_{diss} = 155.2 kJ mole^{-1} (37.1 kcal mole^{-1}). This value is less than the calculated one. Koroban et al. [39] and Williams and Brill [40] obtained ammonium nitroformate (ANF) as a product of HNF decomposition. Enthalpy of ANF dissociation, 164.77 kJ mole^{-1} (39.38 kcal mole^{-1}), is less than that of HNF and agrees closely with the experimental value. Based on this fact, the surface temperature of burning HNF was proposed in Ref. [41] to be determined by dissociation of ANF as a product of the condensed-phase reaction. Temperature dependence of pressure above the burning surface of HNF is given in Table 1.

Vapor pressure above solid HMX was experimentally obtained in Refs. [28,42,30], which led to the heat of sublimation of 161.1–161.9 kJ mole^{-1} (38.5–38.7 kcal mole^{-1}). Before melting HMX undergoes β to δ modification transition with the heat of 9.83 kJ mole^{-1} (2.35 kcal mole^{-1}) [43]. Because of rapid decomposition at the melting point, direct measurements of heat of melting are difficult to conduct. Using indirect measurements, a value 69.9 kJ mole^{-1} (16.7 kcal mole^{-1}) was obtained from the HMX–RDX melting-point diagram [44], while a considerably less value was measured in Ref. [45] as the heat of dissolution of HMX in an inert solvent. The heats of dissolution in acetone, buthylacetate, and aniline were close each other and equal to ∼26.4 kJ mole^{-1} (6.3 kcal mole^{-1}). A close value of HMX melting heat, 34.89 kJ mole^{-1} (8.34 kcal mole^{-1}), was used also in Ref. [44]. In the present work, based on the heat of HMX melting, the heat of phase change, and the heat of sublimation, a value 117.1 kJ mole^{-1} (28 kcal mole^{-1}) was adopted as the heat of HMX evaporation. Starting from this figure and numerous converging data on the surface temperature at atmospheric pressure, 377–380 °C, a pressure dependence of HMX surface temperature was constructed in Ref. [47]. It is presented in Table 1 and Fig. 4.

We failed to find experimental data on heats of neither evaporation nor sublimation for bicyclo-HMX, but the similarity in the HMX and bicyclo-HMX molecular structures suggested the close phase-change heats. Indeed, the surface temperatures of bicyclo-HMX [48] practically coincide with those of HMX [47], and the $P(T_s)$ dependence gives the same heat of evaporation, 117.1 kJ mole^{-1} (28 kcal mole^{-1}) (Table 1 and Fig. 4).

We also failed to find experimental data on heats of neither evaporation nor sublimation for CL-20, heat of sublimation can be calculated only. According to work [55], it is 168.6 kJ mole^{-1} (40.3 kcal mole^{-1}); if using enthalpies of CL-20 formation, calculated for the gas state $\Delta H_f^0 = 590$ kJ mole^{-1} (141 kcal mole^{-1}) [56] and experimental for the solid state $\Delta H_f^0 = 403.3$ kJ mole^{-1} (96.4 kcal mole^{-1}) [57], the enthalpy of sublimation is 186.6 kJ mole^{-1} (44.6 kcal mole^{-1}). Neither DSC curves published, nor our thermocouple records during combustion reveal CL-20 melting phenomenon. However, in the temperature interval between 150 and 190 °C, ε-polymorph of hexanitrohexaazaisowurtzitane transforms to the γ phase by an endothermic transition. The DSC heat of transition calculated from integrated area of the measured endothermic response was found to be 16.52 kJ mole^{-1} (3.95 kcal mole^{-}1) [58], 18.0 kJ mole^{-1} (4.3 kcal mole^{-}1) [59], or 21.46 kJ mole^{-1} (5.13 kcal mole^{-}1) [60]. Thus, heat of CL-20 sublimation at the burning surface may range from 147.3 to 169.5 kJ mole^{-1} (35.2–40.5 kcal mole^{-1}). Based on thermocouple measurements data, value of 120.5 kJ mole^{-1} (28.8 kcal mole^{-1}) was proposed previously [61]. However, it can be assumed from the above considerations that this value is understated one. Thermocouple data of work [62] as well as ours are well described by a line with the slope ratio of 147.3/R, where R is 8.314 kJ mole^{-1} (see Fig. 5).

The pressure dependence of CL-20 burning rate reveals a bend at 1 MPa; the pressure exponent n in the ballistic law $r_b = Bp^n$ changes from 0.68 to 0.79 [61]. Such a change in the pressure exponent for condensed-phase combustion model is obviously connected

with a sharp change in thermophysic and kinetic parameters of the condensed phase. One can assume that CL-20 burning surface temperature grows with pressure and reaches the melting point at 1 MPa. From this assumption, one can calculate the temperature dependence of vapor pressure above liquid CL-20. The dependence shown in Table 1 and Fig. 5 was obtained using estimated heat of CL-20 melting as 38.5 kJ mole^{-1} (9.2 kcal mole^{-1}), which is close to the heat of dissolving of CL-20 in nitroglycerine, 34.5 kJ mole^{-1} (8.25 kcal mole^{-1}) [63]. The dependence was used for obtaining decomposition parameters from burning rate data at pressures above 1 MPa.

Deriving dependence of the surface temperature on pressure for AP involves certain difficulties. First, finding the surface temperature is complicated by not only a very steep temperature rise in profiles to a maximum value, but also high temperature oscillations in the near-to-surface zone. In contrast to pure substance, mixtures of AP with fuels readily reveal characteristic breaks on the temperature profiles that correspond to surface temperatures. Second, it is rather difficult to establish whether AP melts at the burning surface. The presence of the liquid phase has been observed in several studies using microphotography of quenched samples [64–66], but it was not well defined whether the liquid layer was produced during melting of the substance or it was an eutectic solution of decomposition products in AP.

The equilibrium gas pressure over the AP solid surface was measured in work [54]. Experimental temperature dependence of gases over solid AP allows dissociation enthalpy, ΔH_{diss} = 240.6 kJ mole^{-1} (57.5 kcal mole^{-1}). ΔH_{diss} of a salt can be also calculated from enthalpies of formation of the salt and gaseous base and acid. This calculation for AP gives 241.8 kJ mole^{-1} (57.8 kcal mole^{-1}), which is in good agreement with the result obtained from the surface temperature–pressure dependence and conform the mechanism of gasification of the salt through the dissociation reaction.

Values of enthalpy from 238 to 251 kJ mole^{-1} (57–60 kcal mole^{-1}) for AP dissociation have been obtained in many studies, however a value of 117–125 kJ mole^{-1} (28–30 kcal mole^{-1}) is also frequent when it has been ignored that one molecule of the salt produces two molecules of gas rather than one. Moreover, the AP dissociation enthalpy so often has been mistakenly taken as the activation energy of AP decomposition, with dissociation process described as a reaction characterized by kinetic parameters.

As with evaporation, the rate of dissociation is determined by heat flux supplied that is in accordance with the first low of thermodynamics:

$$m = I_{abs}\left[\int_{T_0}^{T_S} cdT + \Delta H_{diss}\right]^{-1},$$

where m is mass evaporation rate, I_{abs} is absorbed heat flux and c is specific heat. The mass evaporation rate of AP subjected to the laser heating flux has been shown in work [67] to depend on the absorbed heat flux in the range from 10 to 100 W/cm^2 as follows:

$$m = \frac{I_{abs}}{k},$$

where k = 3347 kJ kg^{-1} (800 cal g^{-1}). This value has a meaning of heat needed to warm up and evaporate the substance. It consists of heat consumed for warming-up the condensed phase to the phase change temperature 513 K, 285.3 kJ kg^{-1} (68.2 cal g^{-1}), heat of phase transition, 87.9 kJ kg^{-1} (21 cal g^{-1}), heat consumed for warming-up the condensed phase to the surface temperature, 468.6 kJ kg^{-1} (112 cal g^{-1}), and heat of AP dissociation, ~2092 kJ kg^{-1} (500 cal g^{-1}). Heat of AP melting is another constituent to be included in the list to make up the balance. Heat of melting 251 kJ kg^{-1} (60 cal g^{-1}) and melting point 820 K were used in work [68]. Using these values one can calculate vapor pressure above liquid AP.

As illustrated in Fig. 6, experimental results obtained in both thermocouple-aided measurements [49–51] and burning surface pyrometry [53] have large scattering. They can be grouped together along two lines that correspondingly describe the equilibrium gas pressure over the solid and melted AP surface (see Table 1).

3.3. Evaluation of kinetic data of energetic materials in the combustion waves

Ammonium perchlorate. AP combustion mechanism has been studied in many works and the leading role of the condensed-phase reactions at pressures to 10–14 MPa is postulated in many researches. The AP surface temperature increases from 880 to 1070 K as pressure increases from the limiting one (~2 MPa) to 6 MPa. The amount of heat required for warming-up the condensed phase to these temperatures is respectively 1129.7–1506.2 kJ kg^{-1} (270–360 cal g^{-1}). Taking into account the heat generated in AP decomposition 1590–1674 kJ kg^{-1} (380–400 cal g^{-1}), 70% and more of AP must decompose in the condensed phase; this is in agreement with experimental results [68–70]. The remaining substance partly dissociates into gaseous perchloric acid and ammonia under the heat transferred back from the gas and partly is carried away from the surface to the high-temperature gas zone with gases produced and undergoes there decomposition and dissociation.

To obtain rate constants of the dominant reaction on combustion of AP, we used the Zeldovich's condensed-phase model (1), data on AP burning rates in the pressure interval of stable combustion 2–6 MPa [66], surface temperatures derived from the generalized expression for gas pressure over the solid or melted AP surface, and took into account heats of phase change and melting, 88 and 251 kJ kg^{-1} (21 and 60 cal g^{-1}) [67], respectively.

The derived results are shown in Fig. 7 in comparison with decomposition kinetics of gaseous perchloric acid [71], initial rates of decomposition of liquid eutectic of AP with guanidine perchlorate [72], and low- and high-temperature AP decomposition in the condensed phase [71]. An excellent agreement is observed between rate constants of the leading reaction in combustion

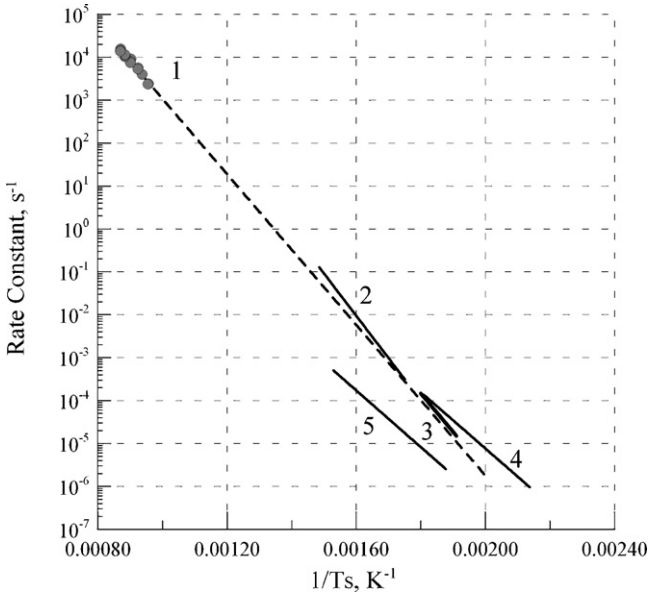

Fig. 7. Rate constants *vs.* reciprocal temperature for the leading reaction on AP combustion (1, points and dashed lines), perchloric acid decomposition in the gas phase (2), initial decomposition of liquid eutectic of AP and guanidine perchlorate (3), AP decomposition in the solid state at low (4) and high temperatures (5).

Table 2
The kinetics parameters of thermal decomposition of studied energetic materials in the combustion wave.

Substance	State of matter	Temperature interval (K)	Equation	Coefficient of determination
AP	Liquid	1045–1150	$k = 10^{11.8}\cdot\exp(-20{,}210/T)$	0.981
AN	Liquid	855–952	$k = 10^{14.4}\cdot\exp(-23{,}754/T)$	0.881
ADN	Liquid	560–705	$k = 10^{16.37}\cdot\exp(-19{,}630/T)$	0.985
HNF	Liquid	550–675	$k = 10^{14.43}\exp(-18{,}400/T)$	0.995
RDX	Liquid	610–800	$k = 10^{15.92}\cdot\exp(-20{,}890/T)$	0.990
HMX	Liquid	660–810	$k = 10^{16.78}\cdot\exp(-23{,}440/T)$	0.994
Bicyclo-HMX	Liquid	650–805	$k = 10^{17.31}\cdot\exp(-23{,}380/T)$	0.998
CL-20	Solid	660–770	$k = 10^{16.55}\cdot\exp(-22{,}870/T)$	0.891
	Liquid	770–960	$k = 10^{15.25}\cdot\exp(-19{,}920/T)$	0.982
NTO	Liquid	630–790	$k = 10^{13.91}\cdot\exp(-19{,}420/T)$	0.995
DAAzF	Liquid	830–1180	$k = 10^{8.66}\cdot\exp(-16{,}680/T)$	0.984

($k = 10^{11.8}\cdot\exp(-20{,}210/T)$) (Table 2), perchloric acid decomposition reaction, and AP initial decomposition in the liquid state. At the same time, these data differ more than three orders of magnitude from the high-temperature decomposition kinetics of AP in solid state. So close agreement with the liquid-state decomposition kinetics provides a convincing evidence for the previously stated assumption on the leading role of chemical processes in thin liquid surface layer on the burning surface of AP.

Ammonium dinitramide. Combustion of ADN has been investigated in many works (see, for example, references in work [20]). Our thermocouple study [20] showed that the lack of heat flux from the gas at least up to 4 MPa allowed considering the condensed-phase chemistry as determining ADN combustion at low pressures. It was proposed that it is ammonium nitrate formed in the decomposition of ADN in the melt, which dissociates from the ADN burning surface, thus controlling the surface temperature.

Rate constants of the dominant combustion reaction of ADN in the pressure range of 0.02–1 MPa were obtained from Zeldovich's expression for the burning rate, taking the surface temperature, T_s, as the AN dissociation one. The average specific heat, c_p, was taken as 2.05 kJ kg^{-1} K^{-1} (0.49 cal g^{-1} K^{-1}), the thermal diffusivity of the condensed phase, χ, as 1.78×10^{-7} m^2 s^{-1} [20], heat of reaction, Q, as 1674 kJ kg^{-1} (400 cal g^{-1} [73]), and heat of melting, L_m, as 14.2 kJ mole^{-1} (3.4 kcal mole^{-1}).

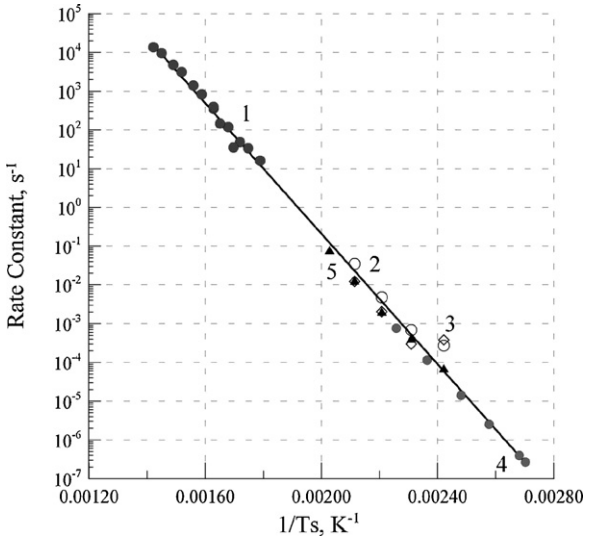

Fig. 8. Rate constants *vs.* reciprocal temperature for the leading reaction on ADN combustion (1) and the kinetics of ADN decomposition found from dinitramide-anion and ammonium-cation disappearance rates (2 and 3 [74]), and from rates of formation of gaseous decomposition products (4 [75] and 5 [74]). Line is drawn through all the points.

As seen in Fig. 8, the results derived from the combustion model, k (s^{-1}) = $10^{16.37}\cdot\exp(-19{,}630/T)$, are in a satisfactory agreement with the ADN decomposition kinetics found by different ways: from dinitramide-anion and ammonium-cation disappearance rates [74], $k = 10^{16.94}\cdot\exp(-20{,}080/T)$ and $k = 10^{15.56}\cdot\exp(-19{,}020/T)$, and from rates of formation of gaseous decomposition products, $k = 10^{14.4}\cdot\exp(-17{,}866/T)$ [75] and $k = 10^{15.4}\cdot\exp(-17{,}765/T)$ [75]. All the data can be described fairly well in the temperature interval of 370–705 K by a general line $k = 10^{16.16}\cdot\exp(-19{,}375/T)$, s^{-1}.

Ammonium nitrate. The decomposition kinetics of liquid AN are described by a first-order equation of autocatalysis [71], with temperature dependence of the constants as follows:

$$k_1 = 10^{14.4}\cdot\exp(-23,754/T),\ \text{s}^{-1} \qquad k_2 = 10^{7.3}\cdot\exp(-5736/T),\ \text{s}^{-1}$$

In view of the conclusions made in Ref. [76] about ionic and radical mechanisms of AN decomposition, it is possible to assume that the constant k_1 describes the radical decomposition pathway with the activation energy corresponding to HO–NO_2 bond rupture; and the constant k_2 describes the low-temperature ionic pathway of decomposition, which also includes side reactions.

Since the activation energy of the self-catalyzed stage is much lower than the activation energy of the initial decomposition reaction, the contribution of self-acceleration is negligible in the field of high temperatures, i.e., at surface temperatures. Autocatalysis can only reduce slightly the activation energy of the overall decomposition.

Pure AN will not burn at all. An addition of some catalysts, fuels or explosives to AN is known to increase strongly its ability to burn. The catalysts and probably carbonaceous fuel capable of forming carbon in pyrolysis, change the AN decomposition kinetics. At the same time, the combustion kinetics of AN mixtures with such capable of burning materials as trinitrotoluene (TNT), methylnitrotetrazole (MNT) and glycidylazidopolymer (GAP), do not change significantly. Although there are different opinions about possible combustion mechanism of AN, our recent thermocouple-aided studies [15,16] clearly indicated that combustion of AN and AN-based mixtures and propellants obeyed the condensed-phase mechanism. Therefore, rate constants of the leading reaction on combustion of AN with energetic materials TNT, MNT and GAP can be evaluated from Eq. (1) (see Fig. 9). This figure presents also kinetic parameters of the leading reaction on combustion of AN with such catalysts as KCl and charcoal.

As can be seen from Fig. 9, combustion of AN mixtures with TNT, MNT and GAP is characterized by rate constants which are close to the decomposition rate constants of neat AN; the influence of autocatalytic reactions is practically absent. Rate constants of the leading combustion reaction of AN with additives of 7% NaCl and 7% charcoal exceed those of the decomposition reaction of neat AN and can be described by straight lines with smaller values of the activation energy of 142–159 kJ mole^{-1} (34–38 kcal mole^{-1}) as

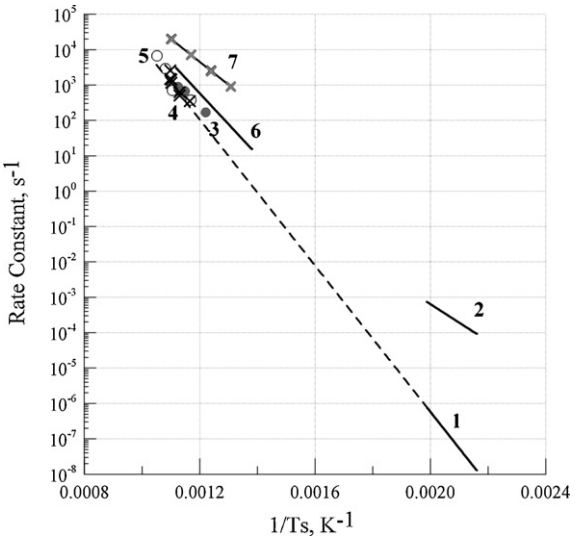

Fig. 9. Comparison of rate constants of decomposition for liquid AN (k_1 (1) and k_2 (2)) with rate constants of the leading reaction on combustion of AN mixtures with 15% MNT (3), 20% TNT (4), 13% GAP (5), 7% KCl (6), and 7% of charcoal (7). Dashed line is extrapolation of k_1.

compared to the activation energy for neat AN as 197.5 kJ mole^{-1} (47.2 kcal mole^{-1}).

The introduction of C1$^-$ ions in AN is known [71] to increase both the initial rate of decomposition (k_1), and the rate of self-acceleration (k_2), with the latter growing much faster than the former. Increase in the degree of self-acceleration results in reduction of the activation energy of the leading combustion reaction of catalyzed AN. Charcoal accelerates autocatalytic reactions of AN decomposition to a greater extent than halides do.

Hydrazinium nitroformate. Kinetic data of HNF decomposition in the condensed phase were obtained by Koroban et al. [39] in isothermal conditions within the temperature interval of 70–100 °C, i.e., below the melting point (E = 169.6 kJ mole^{-1} or 40.5 kcal mole^{-1} and $A = 10^{17.6}$ s^{-1} for the initial decomposition; E = 144.8 kJ mole^{-1} or 34.6 kcal mole^{-1}, $A = 10^{16.1}$ s^{-1} for autocatalysis) and also by Williams and Brill [40] in non-isothermal, "combustion like" conditions in the range of 130–400 °C (E = 104.6 kJ mole^{-1} or 25 kcal mole^{-1}, $A = 10^{11.03}$ s^{-1}). Decomposition parameters were also published by Klerk et al. [77], Winngborg et al. [78] and Bonh [79] (E = 139 kJ mole^{-1} or 33.3 kcal mole^{-1} and $A = 10^{13}$ s^{-1}).

The mechanism of HNF transformation in the condensed phase has been advanced in work [38] and suggested that HNF decomposition process comprised the nitroform decomposition reaction with high activation energy and concurrent reactions of lower activation energy between radicals formed in nitroform destruction and hydrazine moieties of neighboring HNF molecules. According to the above mechanism, the heat produced by the total reaction is estimated as Q = 1674 kJ kg^{-1} (400 cal g^{-1}). A considerable amount of heat capable of generating in the HNF condensed phase is also attested by the ability of HNF to sustain its burning at low pressures in the absence of the gas flame.

The flame structure of HNF has been first investigated fully with thin tungsten–rhenium thermocouples in works [38,41]. The extent to which the decomposition reaction proceeds in the condensed phase can be found from the heat balance at the burning surface [38]. Based on obtained data it was shown that the heat flux from the gas phase totally consumed to evaporation of undecomposed HNF.

Rate constants of the dominant combustion reaction in the pressure range of 0.04–1 MPa were obtained from the Zeldovich's expression, taking the surface temperature as the ANF dissociation temperature. The average specific heat was taken as 1.67 kJ kg^{-1} K^{-1} (0.4 cal g^{-1} K^{-1}), the thermal diffusivity of the condensed phase as 1.35×10^{-7} m^2 s^{-1} [38], density of sample as 1.74 g cm^{-3} and heat of melting as 11.3 kJ mole^{-1} (2.7 kcal mole^{-1}).

As illustrated in Fig. 10, the results derived from the combustion model, $k = 10^{14.43} \cdot \exp(-18{,}400/T)$, s^{-1}, are in satisfactory agreement with the rate constants of the HNF decomposition obtained in works [79,39,78]. Data points obtained from the combustion model fall on the line through data [79] extrapolated to the high-temperature area.

Decomposition data obtained in works [40,77] differ considerably from data of works [39,78,79,38], connected, perhaps, to some methodical mistakes of measurement of the decomposition rate.

Nitramines. An analysis of the burning behavior of well-known cyclic nitramines has shown that variations in the nitramine molecular structure, which increased thermal decomposition rate, resulted in a simultaneous increase in the burning rate [48,80,81]. It is obvious that the molecular structure of the series of cyclic nitramines can exert primary influence on physico-chemical properties and decomposition kinetics of the materials rather than kinetics of redox reactions occurring in the flame. Moreover, the bicyclo-HMX and CL-20 are capable of sustained burning in the lack of the high-temperature gas flame [48,61]. Therefore, with the surface temperatures experimentally determined, rate constants of the first-order leading reactions on combustion of four nitramines, HMX, RDX, bicyclo-HMX, and CL-20 at low pressures, can be derived from the condensed-phase combustion model [3].

In the calculations for HMX, the average specific heat, thermal conductivity, λ, and density of sample, were taken as 1.8 kJ kg^{-1} K^{-1} (0.43 cal g^{-1} K^{-1}), 2.6×10^{-2} kJ s^{-1} m^{-1} K^{-1} (6.3×10^{-4} cal s^{-1} cm^{-1} K^{-1}), and 1.75 g cm^{-3}, respectively. According to DSC studies, heat of reaction in the melt at fast heating, Q, is equal 1387 kJ kg^{-1} (331.5 cal g^{-1}) [82] or 1387 kJ kg^{-1} (331.3 cal g^{-1}) [83]. Heat effect calculated from the composition of reaction products ranges from 805.4 kJ kg^{-1} (192.5 cal g^{-1}) for decomposition in vacuum [47] to 1121.7 kJ kg^{-1} (268.1 cal g^{-1}) for decomposition under atmospheric pressure [84]. Heat of decomposition was assumed variable in the pressure interval 0.03–10 MPa as Q (kJ kg^{-1}) = 1339 + 83.4·ln P. The heat of phase transition was taken as 44.8 kJ mole^{-1} (10.7 kcal mole^{-1} or 36.1 cal g^{-1}); this value

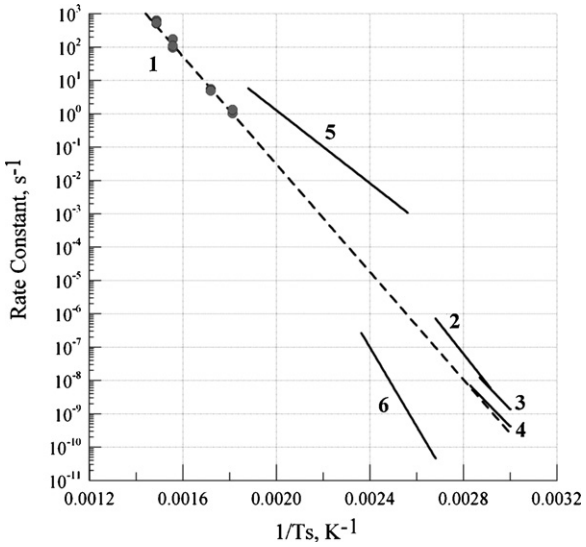

Fig. 10. Comparison of rate constants of the leading reaction on HNF combustion (1, points and dashed line) and rate constants of HNF decomposition: (2) [39], (3) [79], (4) [78], (5) [40], and (6) [77].

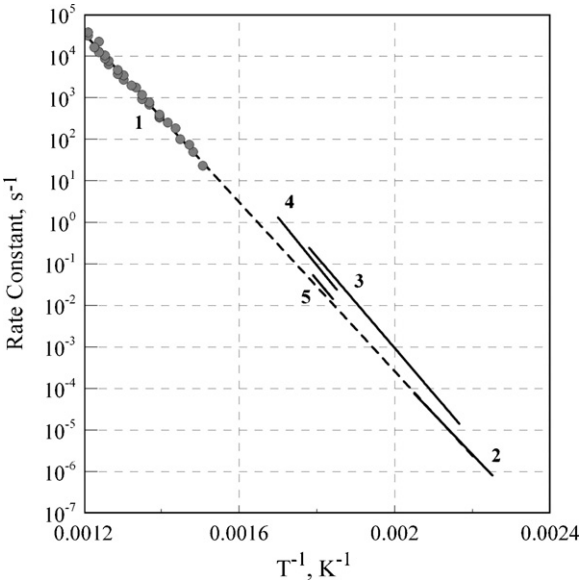

Fig. 11. Comparison of kinetic parameters of the leading reaction of HMX combustion (1, points and dashed line) and decomposition in the solutions of dinitrobenzene (2 [85]), acetone (4 [86]), and in melt (3 [87] and 5 [88]).

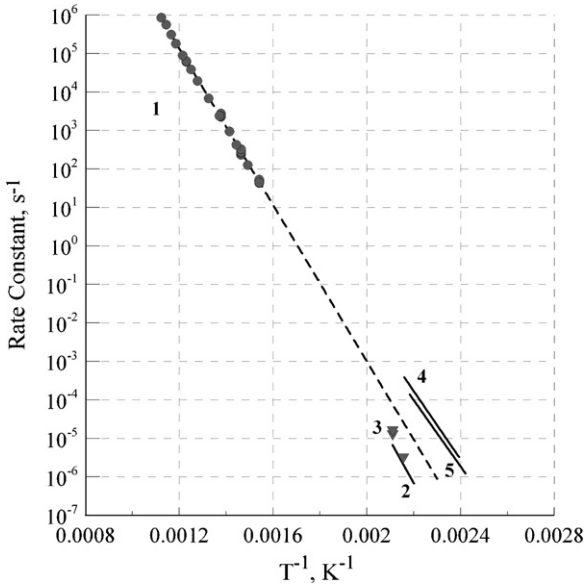

Fig. 12. Comparison of kinetic parameters of the leading reaction of bicyclo-HMX combustion (1) and thermal decomposition in solutions of dibutylphtalate (2, solid and dashed lines) and dinitrobenzene (3, solid line) [89].

included heat of melting, L_m (26.3 kJ mole^{-1} or 6.3 kcal mole^{-1} [45], 32.1 kJ mole^{-1} or 7.67 kcal mole^{-1} [33], and 34.9 kJ mole^{-1} or 8.34 kcal mole^{-1} [46]) and heat of β → δ polymorph phase transition (9.8 kJ mole^{-1} or 2.35 kcal mole^{-1} [43]). For bicyclo-HMX all parameters of the equation were taken as for HMX. Heat of melting and sample density were 33.5 kJ mole^{-1} (8 kcal mole^{-1}) and 1.75 g cm^{-3}, respectively.

In the calculations for RDX, c_p, λ and ρ were taken as 1.59 kJ kg^{-1} K^{-1} (0.38 cal g^{-1} K), 2.3×10^{-2} kJ s^{-1} m^{-1} K^{-1} (5.6×10^{-4} cal s^{-1} cm^{-1} K^{-1}) [90], and 1.75 g cm^{-3}, respectively. According to DSC studies, heat of reaction in the melt is equal to 1080 kJ kg^{-1} (258 cal g^{-1}) [82]. Heat of melting was taken as 33.1 kJ mole^{-1} (7.9 kcal mole^{-1} or 35.6 cal g^{-1}) [33].

In the calculations for CL-20, c_p, λ, and ρ were taken as 1.0 kJ kg^{-1} K^{-1} (0.24 cal g^{-1} K^{-1}) [62], 6.7×10^{-3} kJ s^{-1} m^{-1} K^{-1} (1.6×10^{-4} cal s^{-1} cm^{-1} K^{-1}) [62], and 1.94 g cm^{-3}, respectively. Based on thermocouple-aided measurements, the heat of reaction in the condensed phase was taken as 711 kJ kg^{-1} (170 cal g^{-1}). According to DSC studies, heat of ε → γ polymorph phase transition is equal to 21.5 kJ mole^{-1} (5.13 kcal mole^{-1} or 11.7 cal g^{-1}) [60].

Figs. 11–14 demonstrate comparative analyses between kinetic parameters of the leading reactions on combustion and thermal decomposition of HMX, RDX, bicyclo-HMX, and CL-20, taken from the literature. HMX decomposition kinetics has been taken for the molten substance [88,87] and its solution [85,86]. As can be seen in Fig. 11, kinetic parameters of HMX decomposition derived from the combustion model, $k = 10^{16.78} \cdot \exp(-23{,}440/T)$, s^{-1} are in a good agreement with the experimental rate constants of HMX decomposition in the melt and solutions obtained at low temperatures.

Experimental points of bicyclo-HMX decomposition derived from the combustion model (Fig. 12) fall on the line $k = 10^{17.31} \cdot \exp(-23{,}380/T)$. Extrapolation to the low-temperature range shows that the decomposition rate of bicyclo-HMX in the melt exceeds the decomposition rate in the solid, but is inferior to that in decomposition in dibutylphtalate and dinitrobenzene solutions [87]. Such discrepancy in the reaction rates observed for decomposition in the same aggregative state is perhaps due to solvent participation in the process.

RDX decomposition kinetics has been taken for the molten substance [86,88,91]. As seen in Fig. 13, kinetic parameters of RDX decomposition derived from the combustion model, $k = 10^{15.92} \cdot \exp(-20{,}890/T)$, s^{-1} are in a good agreement with the experimental rate constants of RDX decomposition in the melt obtained at low temperatures.

In the case of CL-20, kinetic data were obtained from monitoring changes in nitro group stretch vibrations in IR spectra [92], from DSC curves at various heating rates [59], and from weight losses in 190–204 °C [92] and 183–211 °C [58] temperature intervals. In the last case, CL-20 decomposition reaction was shown to proceed with pronounced self-acceleration and could be described by a first-order autocatalysis kinetic equation. Besides, Fig. 14 comprises data on decomposition of CL-20 solutions in dinitrobenzene and acetone. As seen from Fig. 14, kinetic parameters of the leading reaction on CL-20 combustion in the pressure interval 0.03–1 MPa ($k = 10^{16.34} \cdot \exp(-22{,}470/T)$, s^{-1}), in

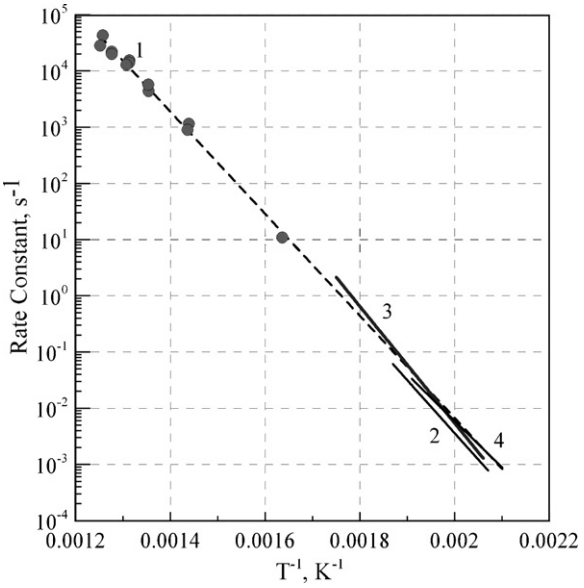

Fig. 13. Comparison of kinetic parameters of the leading reaction on RDX combustion (1, points and dashed line) and decomposition in the melt (2 [91], 3 [88], and 4 [86]).

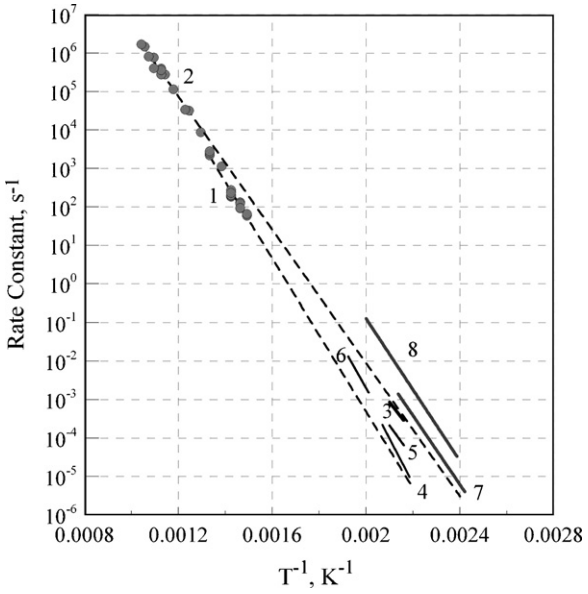

Fig. 14. Comparison of kinetic parameters of the leading reaction on CL-20 combustion in solid phase (1, points and dashed line), liquid phase (2, points and dashed line) and kinetic parameters decomposition (3–8), obtained from IR spectroscopy data (3 [92]), weight loss data (5 [92], 4 [93]), and DSC data (6 [57]). Lines 7 and 8 are temperature dependences of constants for initial rates of decomposition in solution of dinitrobenzene (7 [93] and acetone (8 [86]).

which the surface temperature is determined by sublimation, are in a good agreement with the decomposition kinetics of solid CL-20.

At the same time, kinetic parameters of the leading reaction on CL-20 combustion at pressures above 1 MPa ($k = 10^{15.25}\cdot\exp(-19{,}920/T)$, s^{-1}), in which the surface temperature is determined by evaporation, are in a good agreement with decomposition kinetics in the liquid state.

Diaminoazofurazan. A study of DAAzF combustion [21] showed that at low pressures the burning rate was governed by the condensed-phase chemistry. This may allow finding DAAzF decomposition rate constants in the liquid state in the high-temperature interval of 600–800 °C using Zel'dovich expression for the condensed-phase combustion, burning rates in the pressure range of 1–15 MPa, and surface temperatures derived from pressure dependence of DAAzF boiling temperature. The average specific heat, thermal diffusivity, and sample density were taken as 1.67 kJ kg^{-1} K^{-1} (0.4 cal g^{-1} K^{-1}), 1.4×10^{-7} m^2 s^{-1}, and 1.67 g cm^{-3}, respectively. The heat of reaction in the melt, *Q*, was taken as 1840 kJ kg^{-1} (440 cal g^{-1} or 86 kcal $mole^{-1}$), and the heat of melting, L_m (35.1 kJ $mole^{-1}$ or 8.4 kcal $mole^{-1}$ or 43 cal g^{-1}) was obtained as the difference between heats of sublimation and evaporation.

As seen in Fig. 15, kinetic parameters of DAAzF decomposition derived from the combustion model, $k = 10^{8.66}\cdot\exp(-16{,}680/T)$, s^{-1} are in a good agreement with the experimental rate constants of DAAzF decomposition in the solution [21] at low temperatures. Using rate constants of DAAzF decomposition derived from the combustion model in the temperature interval of 600–800 °C and data on the DAAzF decomposition in solution at low temperatures, one can easily calculate the kinetics of DAAzF decomposition in the widened temperature interval (250–800 °C): $k = 10^{7.61}\cdot\exp(-15{,}570/T)$, s^{-1}. The activation energy of DAAzF decomposition in the liquid state in this temperature interval is 129.4 kJ $mole^{-1}$ (32.9 kcal $mole^{-1}$).

Nitrotriazolone. Thermal decomposition of NTO was studied in a number of works (see, for example, references in work [22]). Such interest was a result of unusual decomposition behavior of NTO connected, as it was shown in work [22], with isomerization of nitro group into the *aci*-form at high temperatures followed by its decomposition.

This circumstance results in two kinetic equations with vastly different activation energies that can be used to describe decomposition of NTO in solid state: in the low-temperature region, $E = 172.0$ kJ $mole^{-1}$ (41.1 kcal $mole^{-1}$), which is characteristic for rupture of C–NO_2 bond, and in the high-temperature region, $E = 322$–368 kJ $mole^{-1}$ (77–88 kcal $mole^{-1}$), a formal value connected with *aci*-isomer decomposition, which concentration grows with temperature.

According to our thermocouple-aided measurements and burning-rate study [22], low values of heat flux from the gas phase at pressures up to at least 2 MPa allow consideration of the condensed-phase chemistry as determining the combustion of NTO. Rate constants of the dominant combustion reaction in the pressure range of 0.4–10 MPa have been obtained from the Zeldovich expression (1). The average specific heat was calculated to be 1.46 kJ kg^{-1} K^{-1} (0.35 cal g^{-1} K^{-1}) from experimental data on thermal diffusivity (1.7×10^{-7} m^2 s^{-1}), strand density was 1.74 g cm^{-3}, and thermal conductivity of the condensed phase was taken from Ref. [96] as 5.1×10^{-2} kJ s^{-1} m^{-1} K^{-1} (0.00123 cal s^{-1} cm^{-1} K^{-1}). The heat of reaction, *Q*, was taken as 1297 kJ kg^{-1} (310 cal g^{-1}) [94], and the heat of melting, L_m, as 215.5 kJ kg^{-1} (51.5 cal g−1) [26].

During combustion, NTO is in the molten state at the surface, having been isomerized into the *aci*-form. Therefore, the kinetics of NTO decomposition derived from the combustion model, $k = 10^{13.91}\cdot\exp(-19{,}420/T)$, s^{-1}, differ from the kinetics of decomposition in solid (Fig. 16). In work [95], decomposition of NTO has been studied in solutions at reduced temperatures; however, it is not obvious if isomerization proceeded to completion at those conditions. At the same time, it is well-known that many salts of nitrocompounds contain the nitro group in the *aci*-form. As seen in Fig. 16, kinetic parameters of NTO decomposition derived from the combustion model are in an excellent agreement with the experimental decomposition rate constants of ethylenediamine and potassium salts of NTO [96] at low temperatures. Decomposition rate constants of a water solution of NTO are also close to rate constants of the leading combustion reaction.

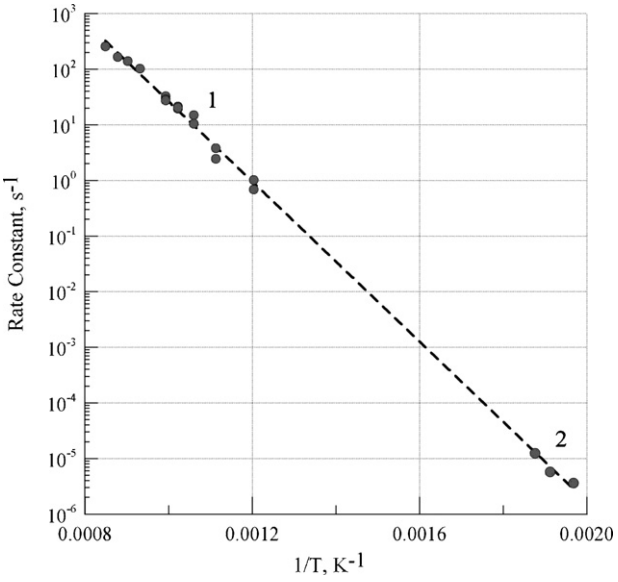

Fig. 15. Comparison of rate constants in a wide temperature interval: rate constants of the leading reaction in DAAzF combustion (1, points and line), rate constants of DAAzF decomposition in solution (2, points).

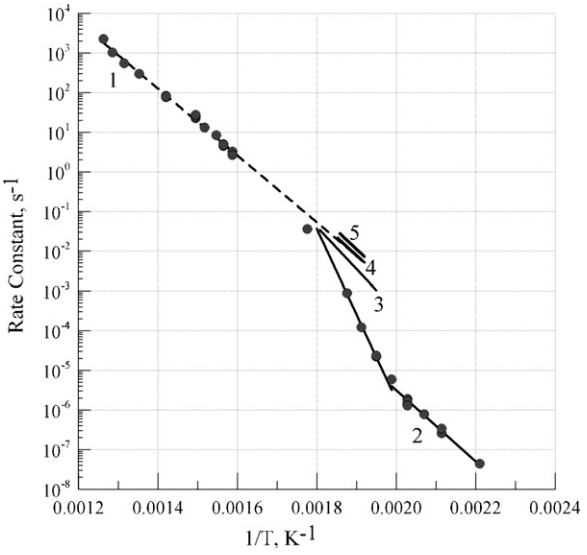

Fig. 16. Comparison of rate constants in a wide temperature interval: the leading reaction in NTO combustion (1, points and line [22]), decomposition of solid NTO (2, points and lines [22]), decomposition of NTO water solution (3 [95]), decomposition of NTO ethylenediamine salt (4 [96]), decomposition of NTO potassium salt (5 [96]).

4. Conclusion

Available experimental data on the burning rates and surface temperatures of a series of energetic materials were used to derive unique kinetic information about decomposition of the materials at high temperatures from the well-known Zeldovich's model for combustion in the condensed phase. Kinetic parameters of the leading reaction on combustion of AP, AN, ADN, HNF, HMX, RDX, bicyclo-HMX and DAAzF thus obtained are in a good agreement with the decomposition kinetics of the substances measured by other techniques at low temperatures. Two sections of the of CL-20 burning rate curve with different pressure exponents allowed calculating decomposition kinetics of the substance in both solid and liquid states. In the case of combustion of AN mixtures with catalysts and charcoal an effect of autocatalysis is observed. Kinetic parameters of NTO decomposition derived from the model appeared to be in a good agreement with experimental decomposition rate constants of potassium and ethylenediamine salts of NTO rather than rate constants of NTO decomposition at low temperature. It was explained by high-temperature isomerization of NTO nitro group into *aci*-form to give the molecular structure like that of NTO salts.

Acknowledgments

This work has been supported by the Ministry of Education and Science of the Russian Federation (project "Development of scientific potential of High School," project code 2.1.2/3781) and Russian Foundation for Basic Research (grant 09-03-00624a).

The authors gratefully acknowledge Dr. Woodward R.H. Waesche for valuable remarks and help in editing of the paper.

References

[1] V.P. Sinditskii, On the nature of the burning rate-controlling reaction of energetic materials for the gas-phase model, Combust. Explos. Shock Waves 43 (3) (2007) 297–308.
[2] S. Zaslonko, V.N. Smirnov, A.M. Tereza, S.A. Tsyganov, Kinetics of energy liberation during thermal decomposition of nitrates in shock waves, Combust. Explos. Shock Waves 24 (2) (1988) 251–255.
[3] Y.B. Zeldovich, Theory of combustion of propellants and explosives, Zh. Eksperimentalnoy i Teoreticheskoi Fiziki 12 (11–12) (1942) 498–524.
[4] A.G. Merzhanov, The theory of stable homogeneous combustion of condensed substances, Combust. Flame 13 (2) (1969) 143–156.
[5] B.V. Novozhilov, The front propagation rate of an exothermic reaction in the condensed phase, Dokl. Akad. Nauk. SSSR 141 (1) (1961) 151–153.
[6] B.I. Khaikin, A.G. Merzhanov, Theory of thermal propagation of chemical reaction front, Combust. Explos. Shock Waves 2 (3) (1966) 22–27.
[7] B.I. Khaikin, A.G. Merzhanov, On combustion of substances with solid reaction layer, Dokl. Akad. Nauk. SSSR 173 (6) (1967) 1382–1385.
[8] A.G. Merzhanov, On role of dispersion in combustion of propellants, Dokl. Akad. Nauk. SSSR 135 (6) (1960) 1439–1441.
[9] V.A. Strunin, On condensed zone of combustion of explosives, Zh. Fiz. Khim. 39 (2) (1965) 433–435.
[10] A.G. Merzhanov, New elementary combustion models of second kind, Dokl. Akad. Nauk. SSSR 233 (6) (1977) 1130–1133.
[11] L.K. Gusachenko, V.E. Zarko, Combustion models for energetic materials with completely gaseous reaction products, Combust. Explos. Shock Waves 41 (1) (2005) 20–34.
[12] A.G. Merzhanov, F.I. Dubovitskii, On the theory of steady state monopropellant combustion, Proc. USSR Acad. Sci. 129 (1959) 153–156.
[13] M.J. Ward, S.F. Son, M.Q. Brewster, Role of gas- and condensed-phase kinetics in burning rate control of energetic solids, Combust. Theor. Model. 2 (3) (1998) 293–312.
[14] A.G. Whittaker, D.C. Barham, Surface temperature measurement on burning solids, J. Phys. Chem. 68 (1) (1964) 196–199.
[15] V.P. Sinditskii, V.Yu. Egorshev, A.I. Levshenkov, V.V. Serushkin, Ammonium nitrate: combustion mechanism and the role of additives, Propell. Explos. Pyrotech. 30 (4) (2005) 269–280.
[16] V.P. Sinditskii, V.Yu. Egorshev, D. Tomasi, L.T. DeLuca, Combustion mechanism of an-based propellants, J. Propul. Power 24 (5) (2008) 1068–1077.
[17] G. Feick, The dissociation pressure and free energy of formation of ammonium nitrate, J. Am. Chem. Soc. 76 (22) (1954) 5858–5860.
[18] J.D. Brandner, N.M. Junk, J.W. Lawrence, J. Robins, Vapour pressure of ammonium nitrate, J. Chem. Eng. Data 7 (2) (1962) 227–228.
[19] A.E. Fogelzang, V.P. Sinditskii, V.Y. Egorshev, A.I. Levshenkov, V.V. Serushkin, V.I. Kolesov, Combustion behavior and flame structure of ammonium dinitramide, Proc. 28th Inter. Ann. Conf. of ICT, Karlsruhe, FRG, 24–27 June, 1997, Paper 90, pp.1–14.
[20] V.P. Sinditskii, V.Y. Egorshev, A.I. Levshenkov, V.V. Serushkin, Combustion of ammonium dinitramide. Part 2. Combustion mechanism, J. Propul. Power 22 (4) (2006) 777–785.
[21] V.P. Sinditskii, M.C. Vu, V.P. Shelaputina, A.B. Sheremetev, N.S. Alexandrova, Study on thermal decomposition and combustion of insensitive explosive 3,3′-diamino-4,4′-azofurazan (DAAzF), Thermochim. Acta 473 (1–2) (2008) 25–31.
[22] V.P. Sinditskii, S.P. Smirnov, V.Y. Egorshev, Thermal decomposition of NTO: explanation of high activation energy, Propell. Explos. Pyrotech. 32 (4) (2007) 277–287.
[23] P.J. Finch, A.J. Gardner, H.S. Head, Majdi, The enthalpies of formation of 1,2,4-triazol-5-one and 3-nitro-1,2,4-triazol-5-one, J. Chem. Thermodyn. 23 (12) (1991) 1169–1173.
[24] J.P. Ritchie, Structures and energies of the tautomers and conjugate bases of some 1,2,4-triazolones, J. Org. Chem. 54 (15) (1989) 3553–3560.
[25] P. Politzer, J.S. Murray, M.E. Grice, Computational determination of heats of formation of energetic compounds, in: T.B. Brill, T.P. Russell, W.C. Tao, R.B. Wardle (Eds.), Decomposition, Combustion and Detonation Chemistry of Energetic Materials, MRS Symp. Proc., vol. 418, 1995, pp. 55–66.
[26] V.L. Zbarsky, A. Basal, N.V. Yudin, V.F. Zhilin, Study on solubility of 2,4-dihydro-1,2,4-triazol-3-one and 5-nitro-2,4-dihydro-1,2,4-triazol-3-one in diluted acid, Proc. 34th Inter. Ann. Conf. of ICT, June 24–27, 2003 Karlsruhe, FRG, Paper 139, pp.1–8.
[27] G.K. Williams, S.F. Potapoli, T.B. Brill, Thermal decomposition of energetic materials 65. Conversion of insensitive explosives (NTO, ANTA) and related compounds to polymeric melon-like cyclic azine burn-rate suppressants, Combust. Flame 98 (3) (1994) 197–204.
[28] J.M. Rosen, C. Dickenson, Vapor pressures and heats of sublimation of some high melting organic explosives, J. Chem. Eng. Data 14 (1) (1969) 120–124.
[29] G. Edwards, The vapor pressure of cyclotrimethylene trinitramine (cyclonite) and pentaerythritoltetranitrate, Trans. Faraday Soc. 49 (1953) 152–154.
[30] R.B. Cundall, T.F. Palmer, C.E.C. Wood, Vapour pressure measurements on some organic high explosives, J. Chem. Soc., Faraday Trans. I 74 (6) (1978) 1339–1345.
[31] Zenin, HMX and RDX: combustion mechanism and influence on modern double-base propellant combustion, J. Propul. Power 11 (4) (1995) 752–758.
[32] Y.-C. Lu, A. Ulas, E. Boyer, K.K. Kuo, Determination of temperature profiles of self-deflagrating RDX by UV/visible absorption spectroscopy and fine-wire thermocouples, Combust. Sci. Technol. 123 (1–6) (1997) 147–163.
[33] S. Zeman, Some predictions in the field of the physical thermal stability of nitramines, Thermochim. Acta 302 (1–2) (1997) 11–16.
[34] N.E. Ermolin, V.E. Zarko, H. Keizers, Analysis of chemical process in the HNF flame, Combust. Explos. Shock Waves 42 (5) (2006) 509–520.
[35] T.S. Kon'kova, Yu.N. Matyushin, Integrated study of the thermochemical properties of nitroformate and its salts, Izv. Akad. Nauk SSSR, ser. khim (12) (1998) 2451–2454.
[36] D. Stull, E.F. Westrum, G. Sinke, The Chemical Thermodynamics of Organic Compounds, J. Wiley, 1969, 865 p.

[37] Y.N. Matyushin, V.P. Lebedev, E.A. Miroshnichenko, L.M. Kostikova, Y.O. Inozemcev, Energy of interaction NO_2-groups in nitroderivatives methane and ethane, Proc. 31st Inter. Annual Conf. of ICT, 2000, 27–30 June, Kalsruhe, FRG, Paper 51, pp.1–8.
[38] V.P. Sinditskii, V.V. Serushkin, S.A. Filatov, V.Yu. Egorshev, Flame structure of hydrazinium nitroformate, in: K.K. Kuo, L.T. DeLuca (Eds.), Combustion of Energetic Materials, Begell House Inc., New York, 2002, pp. 576–586.
[39] V.A. Koroban, T.I. Smirnova, T.N. Bashirova, B.S. Svetlov, Kinetics and mechanisms of the thermal decomposition of hydrazine trinitromethane Trudy MKhTI imeni D. I. Mendeleeva, vol. 104, 1979, pp. 38–44.
[40] G.K. Williams, T.B. Brill, Thermal decomposition of energetic materials 67. Hydrazinium nitroformate (HNF) rates and pathways under combustionlike conditions, Combust. Flame 102 (1995) 418–426.
[41] V.P. Sinditskii, V.V. Serushkin, V.Yu. Egorshev, S.A. Filatov, Combustion mechanism of hydrazinium and ammonium salts of nitroform, in: Chemical Physics of Combustion and Explosion, Proc. XII Symp. on Combustion and Explosion, Part 1, Chernogolovka, 11–15 September, 2000, pp. 141–143.
[42] J.W. Taylor, R.J. Crookes, Vapour pressure and enthalpy of sublimation of 1,3,5,7-tetranitro-1,3,5,7-tetraazacyclooctane (HMX), J. Chem. Soc., Trans. I 72 (1976) 723–729.
[43] P.G. Hall, Thermal decomposition and phase transitions in solid nitramines, Trans. Faraday Soc. 67 (3) (1971) 556–562.
[44] Yu.Ya. Maksimov, Boiling point and enthalpy of evaporation of liquid hexogen and octogen, Russ. J. Phys. Chem. 66 (2) (1992) 280–281.
[45] P. Korobko, I.V. Levakova, S.V. Krasheninnikov, S.I. Drozd, E.A. Butenko, T.A. Bestuzheva, N.I. Shishov, Solubility of nirocompounds in active binder based on polyetherurethane rubber and nitroglycerin, Vooruzhenie. Politika. Konversiya. 5 (41) (2002) 69–74.
[46] E.B. Washburn, M.W. Beckstead, Modeling multiphase effects in the combustion of HMX and RDX, J. Propul. Power 22 (5) (2006) 938–946.
[47] V.P. Sinditskii, V.Y. Egorshev, M.V. Berezin, V.V. Serushkin, Combustion mechanism of HMX in wide pressure range, Combust. Explos. Shock Waves 45 (4), 128–146.
[48] V.P. Sinditskii, V.Y. Egorshev, M.V. Berezin, Study on combustion of new energetic nitramines, Proc. 32th Inter. Ann. Conf. of ICT, Karlsruhe, FRG, July 3–6, 2001, Paper 59, pp.1–12.
[49] N.N. Bakhman, Yu.S. Kichin, S.M. Kolyasov, A.E. Fogelzang, Investigation of the thermal structure of the burning zone in condensed mixtures by fine thermocouples, Combust. Flame 26 (1976) 235–247.
[50] A.J. Sabadell, J. Wenograd, M. Summerfield, Measurement of temperature profiles through solid-propellant flames using fine thermocouples, AAIA J. 3 (9) (1965) 1580–1584.
[51] A.A. Zenin, A.P. Glazkova, O.I. Leipunsky, V.K. Bobolev, Effect of aluminum on the burning of ammonium perchloratepolyformaldehyde mixtures, Combust. Explos. Shock Waves 4 (3) (1968) 165–168.
[52] M. Servieri, L. Galfetti, L.T. De Luca, V.Yu. Egorshev, B.N. Kondrikov, I.V. Grebenyuk, Burning mechanism of composite propellants, Proc. 33th Inter. Ann. Conf. of ICT, Karlsruhe, FRG, 25–28 June 2002, Paper V7, pp. 1–14.
[53] J. Powling, W.A.W. Smith, The Surface temperature of burning ammonium perchlorate, Combust. Flame 7 (3) (1963) 269–275.
[54] S.E. Inami, W.A. Rosser, B. Wise, Dissociation pressure of ammonium perchlorate, J. Phys. Chem. 67 (1963) 1077–1079.
[55] S. Zeman, M. Krupka, Some predictions of the heats of fusion, heats of sublimation, and lattice energies of energetic materials, in: Proc. IV Seminar New Trends in Research of Energetic Materials, Pardubice, Czech Republic, April 11–12, 2001, pp. 393–401.
[56] L. Osmont, I. Catoire, V. Gokalp, Yang, Ab initio quantum chemical prediction of enthalpies of formation, heat capacities, and entropies of gas-phase energetic compounds, Combust. Flame 151 (2007) 262–273.
[57] H. Finck, Graindorge, New molecules for high energetic materials, Proc. 27th Inter. Ann. Conf. of ICT, 1996, Paper 23, pp. 1–5.
[58] S. Lobbecke, M.A. Bohn, A. Pfeil, H. Krause Thermal behavior and stability of HNIW (CL 20), Proc. 29th Inter. Ann. Conf. ICT, June 30–3, 1998, Karlsruhe, FRG, Paper 145, pp. 1–15.
[59] R. Turcotte, M. Yachon, Q.S.M. Kwok, R. Wang, D.E.G. Jones, Thermal study of HNIW (CL-20), Thermochim. Acta 433 (2005) 105–115.
[60] T.P. Russell, P.J. Miller, G.J. Piermarini, S. Block, Pressure/temperature phase diagram of hexanitrohexaazaisowurtzitane, J. Phys. Chem. 97 (1993) 1993–1997.
[61] V.P. Sinditskii, V.Yu. Egorshev, M.V. Berezin, V.V. Serushkin, Yu.M. Milyokhin, S.A. Gusev, A.A. Matveev, Combustion behavior of high energy caged nitramine hexanitrohexaazaisowurtzitane, Zh. Khim. Fiziki 22 (7) (2003) 64–69.
[62] J. Hommel, J.-F. Trubert, Study of the condensed phase degradation and combustion of two new energetic charges for low polluting and smokeless propellants: HNIW and ADN, Proc. 33 Inter. Ann. Conf. ICT, FRG, June 25–28, 2002, Paper V10, pp.1–17.
[63] A.P. Korobko, I.V. Levakova, S.V. Krasheninnikov, S.I. Drozd, E.A. Butenko, T.A. Bestuzheva, N.I. Shishov, Solubility of CL-20 in phlegmatizied nitroglycerin, in: Proc. 3rd All-Russian Conf. Modern Problem of Pyrotechnics, Sergiev Posad, 20–22 October 2004, Ves' Sergiev Posad, 2005, pp. 218–220.
[64] J.D. Hightower, E.W. Price, Combustion of ammonium perchlorate, in: Proc. 11th Symposium of Combustion, Comb. Inst., Baltimore, MD, 1967, pp.463–472.
[65] M.W. Beckstead, J.D. Hightower, Surface temperatures of deflagrating ammonium perchlorate crystals, AIAA J. 5 (10) (1967) 1785–1790.
[66] T.L. Boggs, Deflagration rate, surface structure and subsurface profile of self-deflagration single crystals of ammonium perchlorate, AIAA J. 8 (5) (1970) 867–873.
[67] M. Hertzberg, I.A. Zlochower, Develatilization wave structures and temperatures for the pyrolysis of polymethylmethacrylate, ammonium perchlorate, and coal at combustion level heat fluxes, Combust. Flame 84 (1991) 15–37.
[68] G. Langelle, J. Duterque, J.F. Trubert, Physico-chemical mechanism of solid propellant combustion, in: K.K. Kuo, L.T. DeLuca (Eds.), Combustion of Energetic Materials, Begell House Inc., New York, 2002, pp. 287–333.
[69] C. Guirao, F.A. Williams, A model for ammonium perchlorate deflagration between 20 and 100 atm, AIAA J. 9 (7) (1971) 1345–1356.
[70] C.F. Price, T.L. Boggs, R.L. Derr, The steady-state combustion behavior of ammonium perchlorate and HMX, AIAA Paper 79-0164, Proc. 17th Aerospace Science Meeting, New Orleans, LA, 15–17 January 1979.
[71] G.B. Manelis, G.M. Nazin, Yu.I. Rubtsov, V.A. Strunin, Thermal Decomposition and Combustion of Explosives and Propellants, Nauka, Moscow, 1996, 223 p. (in Russian).
[72] Yu.I. Rubtzov, A.I. Ranevskii, G.B. Manelis, Kinetics of thermal decomposition of ammonium and guanidinium perchlorate mixture, Zh. Fiz. Khimii 44 (1) (1970) 47–51.
[73] A.I. Kazakov, Yu.I. Rubtsov, L.P. Andrienko, G.B. Manelis, Kinetics of the thermal decomposition of dinitramide. 3. Kinetics of the heat release at ADN thermolysis in the liquid phase, Russ. Chem. Bull. 47 (3) (1998) 379–384.
[74] J.C. Oxley, J.L. Smith, W. Zheng, E. Rogers, M.D. Coburn, Thermal Decomposition studies on ammonium dinitramide (ADN) and ^{15}N and ^{2}H isotopomers, J. Phys. Chem. A 101 (1997) 5646–5652.
[75] G.B. Manelis, Thermal decomposition of dinitramide ammonium salt, Proc. 26th Inter. Ann. Conf. ICT, Karlsruhe, 4–7 July, 1995, Paper 15, pp. 1–17.
[76] K.R. Brower, J.C. Oxley, M.P. Tewari, Evidence for homolytic decomposition of ammonium nitrate at high temperature, J. Phys. Chem. 93 (10) (1989) 4029–4033.
[77] W.P.C. de Klerk, A.E.D.M. van der Heijden, W.H.M. Veltmans, Thermal analysis of the high energetic material HNF, J. Therm. Anal. Calorim. 64 (2001) 973–985.
[78] N. Wingborg, M. van Zelst, Comparative study of the properties of ADN and HNF, Report FOA-R-00-1423-310-SE, June 2000.
[79] M.A. Bohn, Thermal stability of hydrazinium nitroformate (HNF) assessed by heat generation rate and heat generation and mass loss, in: Proc. 5th Inter. Symposium on the Heat Flow Calorimetry of Energetic Materials, Naval Surface Warfare Center, Crane, Indiana. September 12 to 14, 2005, Indianapolis, IN, USA, 2005.
[80] V.P. Sinditskii, V.Yu. Egorshev, M.V. Berezin, Combustion of new cyclic energetic nitramines: flame structure and kinetics of leading reaction, in: Proc. 5th Inter. Autumn Seminar on Propellants, Explosives and Pyrotechnics, Guilin, China, October 15–18, 2003, pp. 415–425.
[81] V.P. Sinditskii, V.Yu. Egorshev, M.V. Berezin, Study on combustion of energetic cyclic nitramines, Zh. Khim. Fiz. 22 (4) (2003) 53–60.
[82] J.-S. Lee, C.-K. Hsu, C.-L. Chang, A study on the thermal decomposition behaviours on PETN, RDX, HNS and HMX, Thermochim. Acta 392–393 (2002) 173–176.
[83] G. Singh, S.P. Felix, P. Soni, Studies on energetic compounds part 28: thermolysis of HMX and its plastic bonded explosives containing estane, Thermochim. Acta 399 (2003) 153–165.
[84] A.A. Paletsky, E.N. Volkov, O.P. Korobeinichev, HMX flame structure for combustion in air at a pressure of 1 atm, Combust. Explos. Shock Waves 44 (6) (2008) 639–654.
[85] Yu.Ya. Maksimov, Thermal decomposition of hexogen and oktogen Theory of Explosives, Trudy of MKhTI im. D.I. Mendeleeva, vol. 53, Vyshaja Shkola, Moscow, 1967, pp. 73–84.
[86] J.C. Oxley, A.B. Kooh, R. Szekers, W. Zhang, Mechanism of nitramines thermolysis, J. Phys. Chem. 98 (28) (1994) 7004–7008.
[87] C.E.H. Baun, Kinetics of the thermal decomposition of N-nitro-compounds, in: W.E. Garner (Ed.), Chemistry of the Solid State (Translated into Russian), Inostrannaja Literatura, Moscow, 1961, pp. 335–353.
[88] A.I.B. Robertson, The Thermal decomposition of explosives. II. Cyclotrimethylenetrinitramine and cyclotetramethylenetetranitramine, Trans. Faraday Soc. 45 (1949) 85–93.
[89] R.S. Stepanov, L.A. Kruglyakova, A.M. Astachov, Kinetics of thermal decomposition of some N-nitramines with two fused five membered cycles, Zh. Obshei Khim. 76 (12) (2006) 2063.
[90] T.P. Parr, D.M. Hanson-Parr, Thermal properties measurements of solid rocket propellant oxidizers and binder materials as a function of temperature, J. Energ. Mater. 17 (1) (1999) 1–47.
[91] R.N. Rogers, G.V. Daub, Scanning calorimetric determination of vapor phase kinetic data, J. Anal. Chem. 45 (1973) 596–600.
[92] D.G. Patil, T.B. Brill, Thermal decomposition of energetic materials, 53. Kinetics and mechanism of thermolysis of hexanitrohexazaisowurtzitane, Combust. Flame 87 (1991) 145–151.
[93] B.L. Korsounskii, V.V. Nedel'ko, T.S. Chukanov, T.S. Larikova, F. Volk, Kinetics of thermal decomposition of hexanitrohexazaisowurtzitane, Russ. Chem. Bull. 49 (5) (2000) 812–818.
[94] D.F. McMillen, D.C. Erlich, C. He, C.H. Becker, D.A. Shockey, Fracture-induced and thermal decomposition of NTO using laser ionization mass spectrometry, Combust. Flame 111 (3) (1997) 133–160.
[95] J.C. Oxley, J.L. Smith, L.-Z. Zun, R.L. McKenney, Thermal decomposition studies on NTO and NTO/TNT, J. Phys. Chem. 99 (25) (1995) 10383–10391.
[96] Y. Xie, R. Hu, C.-Q. Yang, G.-F. Feng, J. Zhou, Studies on the critical temperature of thermal explosion for 3-nitro-1,2,4-triazol-5-one (NTO) and its salts, Propell. Explos. Pyrotech. 17 (1992) 298–302.